When is spontaneous formation of spatial patterns robust?

Vit Piskovsky*
Wolfson Centre for Mathematical Biology, Mathematical Institute, University of Oxford, Woodstock Road, Oxford, OX2 6GG and Sir William Dunn School of Pathology, University of Oxford, South Parks Road, Oxford, OX1 3RE

Philip K. Maini
Wolfson Centre for Mathematical Biology, Mathematical Institute, University of Oxford, Woodstock Road, Oxford, OX2 6GG
(Dated: June 11, 2025)

From atomic spins in magnets to galaxies, and from embryonic development to patchy vegetation in arid environments, the physical world is filled with complex systems that spontaneously form spatial patterns. While simple mathematical models, such as reaction-diffusion systems, can explain the formation of such patterns, the complexity of the physical systems these models aim to describe necessitates the analysis of model robustness. Our work utilizes random matrix theory to provide arguably the first definition of robustness that is analytically tractable, providing an easy guide for identifying spatial interactions that robustly generate spatial patterns. We illustrate our theory on examples from mathematical biology, showing that diffusion alone cannot robustly generate spatial Turing patterns in large and unstructured systems, while advection, chemotaxis and non-local interactions can robustly promote pattern formation. Furthermore, we use our theory to prove that the spinodal decompositon of soft condensed matter is dynamically robust and predict the dynamics beyond regimes permitted by the standard Landau-Ginzburg theory. By classifying different spatial interactions based on the robustness of pattern formation, this work provides insights into which mechanisms are fundamental for pattern formation in large and unstructured physical systems.

Spatial patterns emerge across all scales of the physical world and their spontaneous formation provides a central theme of scientific study. The spins of atoms self-organize in magnetic materials [1, 2], reacting chemicals spontaneously form patterns [3], bacterial cells create spatially heterogeneous biofilms [4], animals develop patterned skin pigmentation [5], vegetation is patchily distributed in arid environments [6], and planets, solar systems and galaxies spontaneously emerged from a relatively homogeneous bulk of energy and matter after the Big Bang [7]. Even though different mechanisms drive pattern formation in these systems, the spontaneous formation of spatial patterns has a similar mathematical structure.

Specifically, these systems are commonly described by $a = 1, \ldots, N$ field variables $n_a(t, \boldsymbol{x})$ that represent the physical quantities of interest, ranging from magnetization, chemical concentrations, biofilm bacteria or vegetation to the matter density in the Universe, at time t and spatial coordinates $\boldsymbol{x} = [x_1, \ldots, x_D]^T$. The dynamics of these variables are often described by equations of the form

$$\partial_t n_a(t, \boldsymbol{x}) = f_a(\mathbf{n}(t, \boldsymbol{x})) + \mathcal{F}_a[\mathbf{n}(t, \boldsymbol{x})], \tag{1}$$

where $\mathbf{n}(t, \boldsymbol{x}) = [n_1(t, \boldsymbol{x}), \ldots, n_N(t, \boldsymbol{x})]$ is a vector of field variables, f_a describes temporal interactions and $\mathcal{F}_a$ describes spatial interactions, that is, $\mathcal{F}_a$ is an operator such that

$$\mathcal{F}_a[\mathbf{n}] = 0 \tag{2}$$

for any spatially homogeneous state $\mathbf{n}(t, \boldsymbol{x}) = \mathbf{n}$ (Fig. 1a). For example, the condition (2) is satisfied if the domain is infinitely large $\boldsymbol{x} \in \mathbb{R}^D$ and

$$\mathcal{F}_a[\mathbf{n}(t, \boldsymbol{x})] = -\nabla \cdot \boldsymbol{\mathcal{G}}_a(\mathbf{n}(t, \boldsymbol{x})), \tag{3}$$

where $\boldsymbol{\mathcal{G}}_a[\mathbf{n}(t, \boldsymbol{x})]$ is a flux vector field. In this case, equation (1) is called a continuity equation, which plays a central role in the theory of electromagnetism [8], fluids [9], astrophysical fluids [10], soft condensed matter [11, 12], quantum mechanics [13], thermodynamics [14], chemical reactions [15] and multiple biological systems [16–18]. With the general formulation of the dynamics in equation (1), spontaneous pattern formation can be studied similarly across diverse physical systems as follows.

Without spatial interactions, $\mathcal{F}_a = 0$, and on infinite domains, $\boldsymbol{x} \in \mathbb{R}^D$, the temporal dynamics in equation (1) commonly admits a stable spatially homogeneous stationary state $\mathbf{n}(t, \boldsymbol{x}) = \boldsymbol{n}^*$, which is given by

$$f_a(\boldsymbol{n}^*) = 0; \quad a = 1, \ldots, N, \tag{4}$$

and is associated with a Jacobian matrix $J^{(0)}_{ab} = \partial f_a / \partial n_b|_{\boldsymbol{n}^*}$ with eigenvalues that all have negative real parts. Importantly, a positive answer to the following question determines spontaneous pattern formation. Is the spatially homogeneous stationary state $\mathbf{n}(t, \boldsymbol{x}) = \boldsymbol{n}^*$ stable when the spatial interactions $\mathcal{F}_a$ are present (Fig. 1b)?

As can be seen in [2–7], this question has sparked attention across different fields of study. Most notably,

* vit.piskovsky@maths.ox.ac.uk

spontaneous pattern formation has been studied intensively in the context of reaction-diffusion systems [16], with a long history tracing back to Alan Turing. In 1952, Turing showed that the diffusion,

$$\mathcal{F}_a[\mathbf{n}(t,\boldsymbol{x})] = d_a \nabla^2 n_a(t,\boldsymbol{x}), \tag{5}$$

of two interacting variables ($N = 2$) with diffusivities $d_a > 0$ can destabilise their temporally stable spatially homogeneous distribution, even though the diffusion of a single self-interacting variable ($N = 1$) cannot do this [19]. In particular, for patterns to form, one variable must diffuse slowly and activate the dynamics, while the other must diffuse quickly and inhibit the dynamics [16]. Despite the simplicity of the proposed Turing mechanism, observing Turing patterns in experimental and natural systems took several decades [20]. Moreover, those systems that admit Turing patterns are often more complex than can be described with two variables, a slow activator and a fast inhibitor. For example, the chemical reactions that admit Turing patterns involve multiple reactants [3, 21, 22] with similar diffusivities [23]. Biofilm patterns are composed of bacteria that interact with complex chemical environments, secrete multiple extracellular polymeric substances and are capable of biased non-diffusive motility [24]. In zebrafish, pigment cells - melanophores and xanthophores - interact with various chemical factors [5] and undergo a non-diffusive movement [25] to produce stripes and spots on the zebrafish skin. The patterns of vegetation in an arid environment are affected by various biotic and abiotic factors [6], and plant seeds can be dispersed non-locally [26], for example by rodents [27]. The inherent complexity of these systems raises an important question. Is diffusion sufficiently robust to explain pattern formation in such complex physical systems [28]?

In principle, there are different aspects of robustness [28], including parametric and structural robustness (Fig. 1c). Pattern formation is said to be robust parametrically when it occurs for a broad range of parameters in the interactions f_a and $\mathcal{F}_a$, while structural robustness requires pattern formation to occur across a broad range of spatial dimensions D and variables N. For diffusion, the analytical conditions for pattern formation were recently derived for $N = 3$ variables and necessary conditions were provided for an arbitrary number of variables N [29]. However, as these conditions are difficult to interpret, several authors have now investigated the robustness of pattern formation with $N \geq 2$ variables numerically [23, 30, 31]. Inspired by Robert May's idea to examine the stability of large complex systems with a random matrix theory approach [32], these works accounted for parametric robustness by sampling interactions randomly and for structural robustness by repeating the calculation for multiple numbers of variables N [23, 31]. Surprisingly, the probability of observing pattern formation in these random systems rapidly decreased with the increasing number of variables N, as has been recently supported by a heuristic analytical argument [33]. In parallel, pattern formation has been analyzed beyond the contexts of diffusion, such as for advection [34], chemotaxis [35], cross-diffusion [36], or non-local interactions [37, 38]. Interestingly, these works often report that such alternative mechanisms promote pattern formation, but the comparison of pattern formation between models with different spatial interactions $\mathcal{F}_a$ is hindered by the absence of a formal and analytically tractable definition of robustness.

In this Letter, we propose arguably the first analytical and systematic approach to quantifying the robustness of pattern formation governed by different spatial interactions $\mathcal{F}_a$. Inspired by random matrix theory, we define pattern formation to be robust if patterns form spontaneously in the considered system when it is large (i.e., includes many variables $N \to \infty$) and unstructured (i.e., has random, independent and identically distributed interactions), allowing us to capture both parametric and structural robustness. Utilizing our new definition and the recent progress in random matrix theory [39, 40], we will provide a simple rule to identify which spatial interactions $\mathcal{F}_a$ are congruent with robust formation of spontaneous patterns (Fig. 1d-e).

To formalize this idea, we use linear stability analysis to determine whether spatial perturbations around a temporally stable homogeneous stationary state $\boldsymbol{n}^*$ can grow, allowing for spontaneous pattern formation [16]. In particular, linearization of equation (1) around the homogeneous stationary state $\boldsymbol{n}^*$ and a subsequent Fourier transformation show that whether or not the spatial perturbations grow on an infinitely large domain $\boldsymbol{x} \in \mathbb{R}^D$ is determined by the eigenvalues of the matrix

$$J_{ab}(\boldsymbol{k}) = \sum_{p=0}^{\infty} \sum_{\{\alpha_1 \ldots \alpha_p\}} J_{ab}^{(p),\alpha_1\ldots\alpha_p} \prod_{q=1}^{p} (ik_{\alpha_q}), \tag{6}$$

where $\boldsymbol{k} = (k_1, \ldots, k_D)$ is a wavenumber vector of the perturbation,

$$J_{ab}^{(p),\alpha_1\ldots\alpha_p} = \left. \frac{\partial \mathcal{F}_a}{\partial \left(\nabla_{\alpha_1} \ldots \nabla_{\alpha_p} n_b \right)} \right|_{\boldsymbol{n}^*} \tag{7}$$

describes different spatial interactions of order $p \geq 1$, and $J_{ab}^{(0)} = \partial f_a / \partial n_b |_{\boldsymbol{n}^*}$ describes the stabilizing temporal interactions and has all eigenvalues with negative real parts. Denoting $\lambda(\boldsymbol{k})$ to be the eigenvalue of $J_{ab}(\boldsymbol{k})$ with maximal real part, it can be noticed that patterns form spontaneously precisely if there exists a perturbation with wavenumber $\boldsymbol{k}^*$ that can grow at a positive rate

$$\mathrm{Re}(\lambda(\boldsymbol{k}^*)) > 0. \tag{8}$$

Moreover, the formation of such patterns is regular if perturbations with infinitely small wavelengths cannot grow, that is if $\mathrm{Re}(\lambda(\boldsymbol{k}))$ is bounded from above by zero as $|\boldsymbol{k}| \to \infty$ (Fig. 1e).

Having identified when patterns form spontaneously and regularly, we can return to our definition of robustness. For simplicity of presentation, we will restrict our

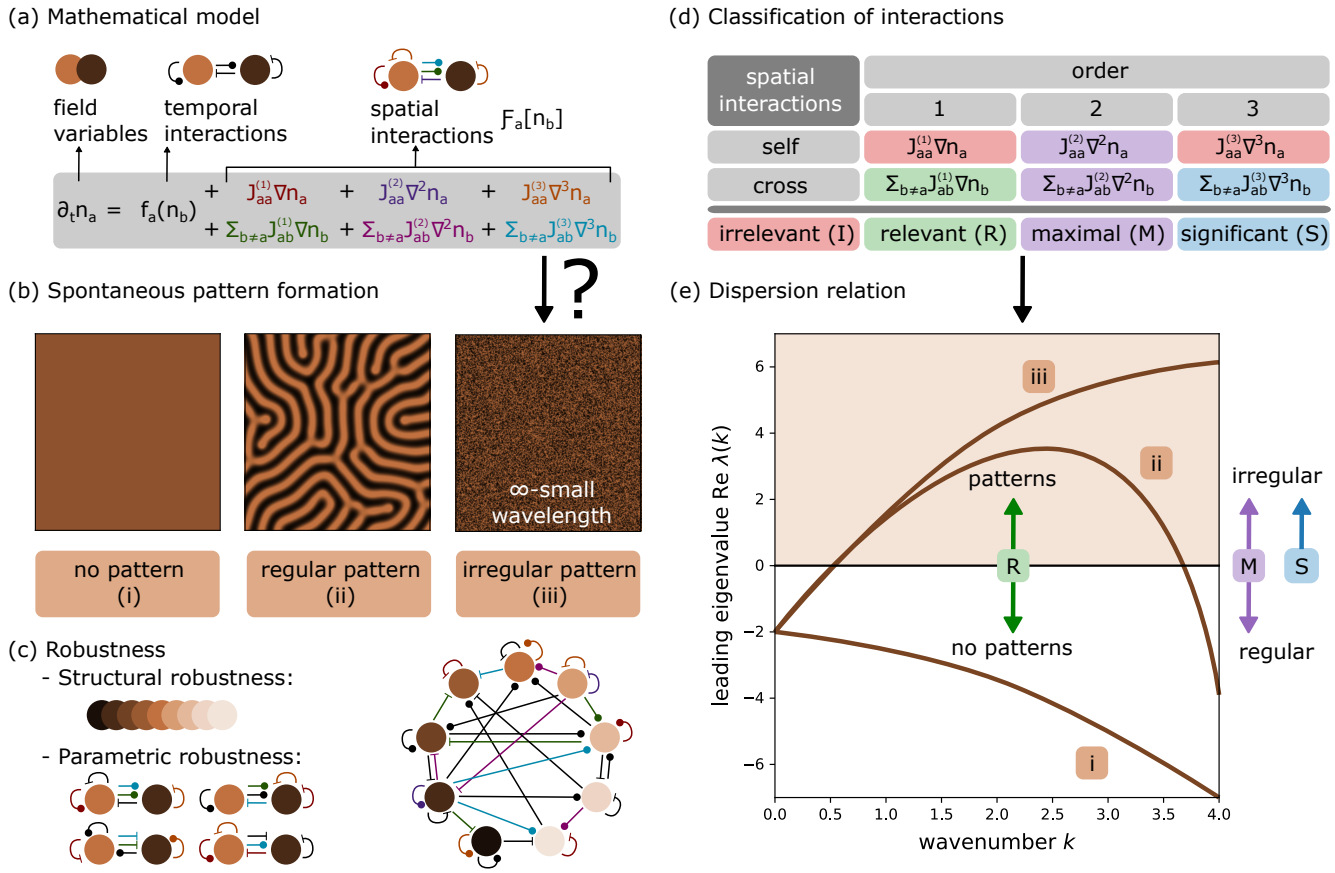

FIG. 1. **Robustness of spontaneous pattern formation.** **(a)** Mathematical model for field variables $n_a(t,x)$ (brown circles) with temporal interactions $f_a(n_b)$ (black connections) and spatial interactions $\mathcal{F}_a[n_b]$ (coloured connections), which are expanded order by order with matrix coefficients $J^{(p)}_{ab}$. **(b)** Spatial patterns form spontaneously if a temporally stable homogeneous stationary state is unstable to spatial perturbations. Several outcomes are possible: (i) no patterns, (ii) regular patterns (with finite wavelengths), and (iii) irregular patterns (with infinitely small wavelengths). **(c)** A key question is whether patterns form robustly in a given model, that is for different numbers N of field variables (structural robustness) and for different parameter values of interactions $J^{(p)}_{ab}$ (parametric robustness). We define pattern formation to be robust if patterns can form spontaneously in a system with many variables $N \to \infty$ and independent random interaction parameters $J^{(p)}_{ab}$. **(d)** To analyze robustness of spatial interactions, different interactions are classified as irrelevant (I, red), relevant (R, green), maximal (M, purple) and significant (S, blue), as explained in Definition 1. **(e)** The dispersion relation captures the growth rate (leading eigenvalue) of perturbations with wavenumber k around the homogeneous stationary state. Therefore, patterns form spontaneously only if some perturbation has a positive growth (brown region) and pattern formation is regular if perturbations with infinitely large wavenumbers have negative growth (white region). Different dispersion relations (brown curves) can be identified with different regimes 1-3 of pattern formation from panel (b). Theorems 1 and 2 explain that relevant interactions influence the robustness of pattern formation, while maximal and significant interactions control its regularity. Coloured arrows indicate changes in the dispersion relation induced by changes in the interaction strength r_p of an interaction from a class in panel (d), see Definition 1.

study to a single spatial dimension ($D = 1$), which allows us to ignore different spatial indices α_q and replace a wavenumber vector $\boldsymbol{k}$ by a single wavenumber k. With the goal to study unstructured systems, we assume that the interactions $J^{(p)}_{ab}$ of order p between variables a and b are sampled randomly and independently for different orders p and different combinations of a and b, with self-interactions ($a = b$) and cross-interactions ($a \neq b$) of the same order p sampled from identical probability distributions, with means and variances given by

$$\begin{aligned} a = b: \ \mathbb{E}\, J^{(p)}_{ab} &= \mu_{sp}, \ \ \mathrm{Var}\, J^{(p)}_{ab} = \sigma^2_{sp}, \\ a \neq b: \ \mathbb{E}\, J^{(p)}_{ab} &= \mu_{cp}, \ \ \mathrm{Var}\, J^{(p)}_{ab} = \sigma^2_{cp}, \end{aligned} \tag{9}$$

where we account for the possibility that the cross-interactions are symmetric ($\tau_p = +1$), neutral ($\tau_p = 0$) or anti-symmetric ($\tau_p = -1$) via [41]

$$\mathrm{Cov}\left(J^{(p)}_{ab}, J^{(p)}_{ba}\right) = \tau_p \sigma^2_{cp}. \tag{10}$$

With this assumption, we can say that an interaction is present in the system if the corresponding mean or

variance are non-vanishing. This allows us to classify the interactions as follows (Fig. 1d).

Definition 1 *Let P be the maximal even order of interactions that are present in the system. Then, we classify the spatial interactions ($p \geq 1$) as*

- *maximal (M): interactions of order P*
- *irrelevant (I): symmetric cross-interactions and self-interactions of any odd order p,*
- *significant (S): cross-interactions of odd order $p > P$ that are not symmetric,*
- *relevant (R): all remaining interactions of order $p < P$.*

For example, if no odd cross-interactions are symmetric, we have:

Order	*1*	*2*	*3*	...	$P-1$	P	$P+1$	$P+2$	$P+3$	...
Self	*I*	*R*	*I*	...	*I*	*M*	*I*	$\varnothing$	*I*	...
Cross	*R*	*R*	*R*	...	*R*	*M*	*S*	$\varnothing$	*S*	...

Moreover, we define the strength r_p of interactions of order $p \geq 0$ by

$$r_p = (\mu_{sp} - \mu_{cp})(-1)^{\frac{p}{2}} + \\ + \sqrt{N} \max\left(\sigma_{cp}\left(1+\tau_p\right), \sqrt{N}\mu_{cp}(-1)^{\frac{p}{2}}\right), \tag{11}$$

when p is even, and by

$$r_p = \sqrt{N}\sigma_{cp}\left(1-\tau_p\right). \tag{12}$$

when p is odd.

The interaction strengths can be used to simplify the subsequent analysis. As shown in Appendix A, the interaction strengths measure whether the matrix $i^p J_{ab}^{(p)}$ has all eigenvalues with negative real parts ($r_p < 0$) or not ($r_p > 0$). For example, the assumption about the stability of the homogeneous stationary state $\boldsymbol{n}^*$ translates to the assumption that $r_0 < 0$.

Having introduced unstructured systems as those with random interactions, we can now formulate our definition of robustness (Fig. 1c).

Definition 2 *We say that spontaneous pattern formation is robust in a system given by equation (1) if the patterns can form spontaneously when the system is large ($N \to \infty$) and unstructured (i.e., has random, independent and identically distributed interactions as in equations (9) and (10)).*

With these definitions, we can now state the main result (Fig. 1e, see Appendix A for proof).

Theorem 1 *Assuming that the variance of the self-interactions is bounded by the variance of cross-interactions (i.e., $\sigma_{sp} \leq C\sigma_{cp}$ for some constant $C > 0$), it is true that:*

1. *When irrelevant interactions are the only interactions present, pattern formation is not robust.*
2. *When at least one significant interaction is present with a non-vanishing strength ($r_p \neq 0$), pattern formation is robust and irregular.*
3. *When all significant interactions have vanishing strength ($r_p = 0$) and the relevant interactions are absent, pattern formation is either not robust ($r_P \leq 0$) or it is robust and irregular ($r_P > 0$), depending on the strength of the maximal interaction r_P.*
4. *When a relevant interaction is present and sufficiently strong ($r_p \gg 0$), pattern formation is robust. Moreover, such pattern formation is regular, provided all significant interactions have vanishing strength ($r_q = 0$) and the maximal interaction has a negative strength ($r_P < 0$).*

Importantly, Theorem 1 allows us to determine whether a particular spatial interaction $\mathcal{F}_a$ in equation (1) forms spontaneous patterns robustly based on a simple inspection of the terms in $\mathcal{F}_a$. For example, if $\mathcal{F}_a$ includes only irrelevant interactions, then Theorem 1 predicts that patterns do not form robustly. One could think that this is a consequence of the additional assumption ($\sigma_{sp} \leq C\sigma_{cp}$ for some constant C) that restricts the heterogeneity of self-interactions to zero when the cross-interactions are absent. While this additional assumption provides a key simplification in the proof of Theorem 1 (see Appendix A), the key propositions of Theorem 1 remain valid even if all cross-interactions are absent (see Appendix B for proof).

Theorem 2 *Assume that the temporal interactions are neutral ($\tau_0, \mu_{c0} = 0$) and that the only spatial interactions present in the system are self-interactions (with arbitrary distribution). Then, the following statements are true:*

1. *When irrelevant interactions are the only interactions present, pattern formation is not robust.*
2. *When the relevant interactions are absent, pattern formation is either not robust ($J_{aa}^{(P)}(-1)^{\frac{P}{2}} \leq 0$ for all a) or it is robust and irregular ($J_{aa}^{(P)}(-1)^{\frac{P}{2}} > 0$ for some a), depending on the maximal interactions $J_{aa}^{(P)}$.*
3. *When a relevant interaction is sufficiently strong ($J_{aa}^{(p)}(-1)^{\frac{p}{2}} \gg 0$ for some a), pattern formation is robust. Moreover, such pattern formation is regular, provided the maximal interactions are negative ($J_{aa}^{(P)}(-1)^{\frac{P}{2}} < 0$ for all a).*

Moreover, it is possible to extend these general results to multiple spatial dimensions, $D > 1$, as outlined in Appendix C.

In the rest of this Letter, we will illustrate the general

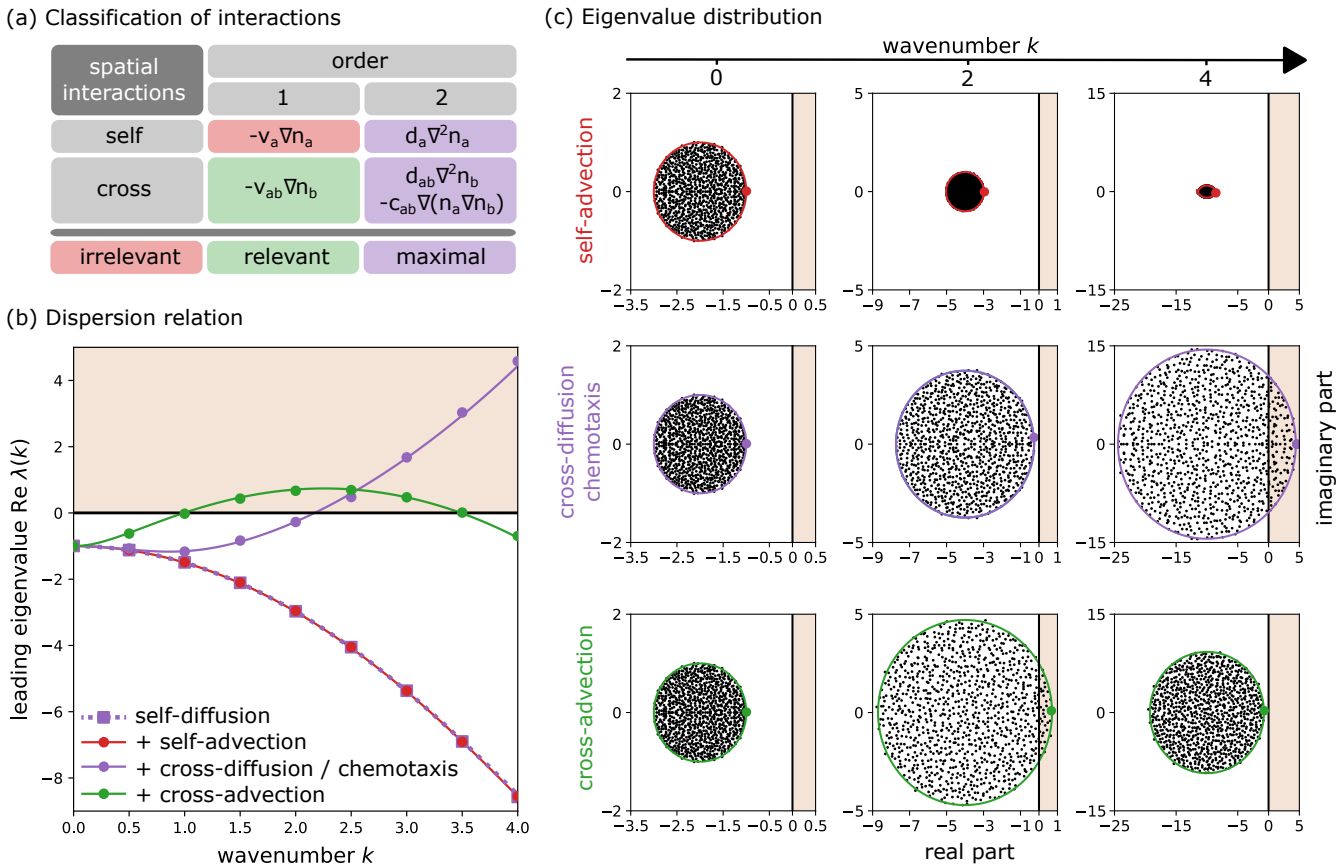

FIG. 2. **Example 1: Reaction-advection-diffusion systems.** **(a)** Interactions in equation (13) are classified as irrelevant (red; self-advection, v_a), relevant (green; cross-advection, v_{ab}), and maximal (purple; self-diffusion, $d_a > 0$; cross-diffusion, d_{ab}; chemotaxis, c_{ab}). A positive self-diffusion ($d_a > 0$) is included in all our systems. **(b)** Dispersion relations for large ($N = 1000$) and unstructured systems ($\tau_p = 0$) with different spatial interactions: self-diffusion alone (purple squares and dotted line), self-diffusion and self-advection (red dots and line), self-diffusion and cross-diffusion/chemotaxis (purple dots and solid line), self-diffusion and cross-advection (green dots and line). Lines correspond to the analytics in equation (A7) (resp. (B2)) if cross-interactions are present (resp. absent). Symbols represent numerical simulations of the Jacobian matrix in equation (14), where entries are sampled independently from Gaussian distributions (resp. a Gamma distribution for $d_a > 0$) with means $\mu_{s0} = -2$, $\mu_{s2} = 0.5$, $\mu_{s1} = \mu_{cp} = 0$ and standard deviations $\sigma_{c0} = \sigma_{sp} = 1/\sqrt{N}$, $\sigma_{c1} = 2.3/\sqrt{N}$, $\sigma_{c2} = 0.9/\sqrt{N}$. The brown region denotes a robust pattern formation. **(c)** Eigenvalues of the simulated Jacobian matrix for wavenumbers $k = 0, 2, 4$ and systems where self-diffusion is enhanced by self-advection (red), cross-diffusion/chemotaxis (purple) and cross-advection (green). Black dots represent all eigenvalues from the numerical simulations in panel (b), coloured dots represent the leading eigenvalues plotted in panel (b), and coloured lines represent the analytics, which are based on the same equations as in panel (b). See Supplemental Material for the Python code.

results on several examples from mathematical biology and soft condensed matter physics. In mathematical biology, the spatial interactions of advection, diffusion and chemotaxis play a key role [16]. With these interactions, the dynamics in equation (1) becomes

$$\begin{aligned}\partial_t n_a = f_a(\mathbf{n}) - v_a\nabla n_a + d_a\nabla^2 n_a - \sum_{b\neq a} v_{ab}\nabla n_b \\ + \sum_{b\neq a} d_{ab}\nabla^2 n_b - \sum_{b\neq a} c_{ab}\nabla(n_a\nabla n_b),\end{aligned} \tag{13}$$

where v_a (resp. v_{ab}) is the velocity of self-advection (resp. cross-advection), d_a (resp. d_{ab}) is the diffusivity of self-diffusion (resp. cross-diffusion) and c_{ab} describes chemotaxis of variable a up the gradient of variable b (Fig. 2a). Upon linearization, we find that these interactions are at most of second order and

$$\begin{aligned} J^{(1)}_{ab} &= \begin{cases} -v_a & \text{if } a = b \\ -v_{ab} & \text{if } a \neq b, \end{cases} \\ J^{(2)}_{ab} &= \begin{cases} d_a & \text{if } a = b \\ d_{ab} - n^*_a c_{ab} & \text{if } a \neq b. \end{cases} \end{aligned} \tag{14}$$

Since the temporal interactions are assumed to be unstructured, the spatially homogeneous stationary state is commonly approximated by $n^*_a = n^*$ for some n^* [40, 42]. Therefore, by sampling the velocities, diffusivities and

chemotactic coefficients independently and from identical distributions, we obtain equation (9) with

$$\begin{aligned} \mu_{s1} &= \mathbb{E}\, v_a, & \mu_{s2} &= \mathbb{E}\, d_a, \\ \mu_{c1} &= \mathbb{E}\, v_{ab}, & \mu_{c2} &= \mathbb{E}\, d_{ab} - n^* \,\mathbb{E}\, c_{ab}, \\ \sigma_{s1}^2 &= \operatorname{Var} v_a, & \sigma_{s2}^2 &= \operatorname{Var} d_a, \\ \sigma_{c1}^2 &= \operatorname{Var} v_{ab}, & \sigma_{c2}^2 &= \operatorname{Var} d_{ab} + (n^*)^2 \operatorname{Var} c_{ab}. \end{aligned} \tag{15}$$

The models in mathematical biology commonly include a positive self-diffusion $d_a > 0$ [16], which implies that $\mu_{s2} > 0$ and the maximal even interaction has order $P = 2$. In particular, as long as cross-advection is not anti-symmetric, the interactions can be classified as in Fig. 2a. By Theorem 2, a system with positive self-diffusion does not give rise to robust pattern formation (Fig. 2b). This result explains why self-diffusion alone cannot generate Turing patterns in large and unstructured random systems, as observed in numerical simulations [23, 31], and it formalizes the previous heuristic argument [33] and extends the previous analytics for homogeneous diffusivity with $\operatorname{Var} d_a = 0$ [43]. In line with Theorem 2, we can also notice that the addition of self-advection into such a system cannot rescue the robustness of pattern formation (Fig. 2b,c). While self-advection cannot promote the robustness of pattern formation, Theorem 1 shows that sufficiently strong cross-diffusion and chemotaxis can generate patterns that are robust but not regular (Fig. 2b,c, Appendix D). This result aligns with the observation that patterns form robustly in the Keller-Segel model of chemotaxis [35], but these patterns blow up in finite time [44, 45]. Finally, Theorem 1 asserts that the only considered spatial interaction that gives rise to the formation of robust and regular patterns is cross-advection (Fig. 2b,c, Appendix D), aligning with the observation that cross-advection can support a variety of spatio-temporal patterns [46]. Overall, these results are consistent with a recent analysis of pattern formation in general reaction-advection-diffusion systems with two variables ($N = 2$), which suggests that cross-interactions facilitate pattern formation more robustly than self-interactions [47].

While the examples from mathematical biology are often limited to spatial interactions of order $p \leq 2$, higher order interactions appear commonly in soft condensed matter, such as fluid mixtures. In this context, spontaneous pattern formation, known as spinodal decomposition, corresponds to a phase transition in which a homogeneously distributed matter spontaneously separates into distinct phases [12]. Due to the inherent complexity of many physical systems [48], multiple studies have examined spinodal decomposition in systems with many components N [48–53]. For example, [52] studied a fluid mixture with $a = 1, \ldots, N$ components. The components were described by volume fractions $n_a(t, x)$, the remaining volume fraction of $1 - \sum_a n_a$ was attributed to the solvent, and the mechanics was described by the free energy functional

$$F = \int \left[\sum_a \frac{\kappa}{2} (\nabla n_a)^2 + g(\boldsymbol{n}) \right] \mathrm{d}x, \tag{16}$$

where $\kappa > 0$ describes a surface tension and

$$\begin{aligned} g(\boldsymbol{n}) = \sum_{a,b} \frac{\chi_{ab}}{2} n_a n_b + \sum_a n_a \ln n_a \\ + (1 - \sum_a n_a) \ln\left(1 - \sum_a n_a\right) \end{aligned} \tag{17}$$

describes the bulk free energy density of the homogeneous state. In equation (17), the symmetric matrix χ_{ab} describes interactions between different components of the mixture and the remaining terms describe the entropy of the mixing. Spinodal decomposition has been examined using Landau-Ginzburg and random matrix theories [52]. Specifically, random matrix theory was used to test whether the Hessian matrix

$$H_{ab} = \frac{\partial^2 g}{\partial n_a \partial n_b} = \chi_{ab} + \frac{\delta_{ab}}{n_a} + \frac{1}{1 - \sum_c n_c} \tag{18}$$

has a negative eigenvalue, that is, whether an appropriate homogeneous perturbation around a homogeneous stationary state $n_a = n_a^*$ can reduce the free energy (Fig. 3a). Assuming that the symmetric interactions χ_{ab} are independent and identically distributed

$$\begin{aligned} a = b: \ \mathbb{E}\, \chi_{ab} = \nu_s, \ \operatorname{Var} \chi_{ab} = \sigma_s^2, \\ a \neq b: \ \mathbb{E}\, \chi_{ab} = \nu_c, \ \operatorname{Var} \chi_{ab} = \sigma_c^2, \end{aligned} \tag{19}$$

and that the homogeneous stationary state is equimolar ($n_a^* = \beta/N$ for some $\beta < 1$), spinodal decomposition occurs precisely when

$$\begin{aligned} 0 < r_2 \equiv -1 + \frac{\beta\,(\nu_c - \nu_s)}{N} + \\ + \max\left(\frac{2\beta\sigma_c}{\sqrt{N}}, \frac{\beta}{\beta - 1} - \beta\nu_c \right), \end{aligned} \tag{20}$$

which coincides with the result in [52] for the restricted case of $\nu_s = \nu_c = \nu$ and $\sigma_{s2} = \sigma_{c2} = \sigma$ (Appendix E). To simulate spinodal decomposition numerically, [52] used the so-called model B, given by

$$\partial_t n_a = \nabla \cdot (M_a \nabla \mu_a) \tag{21}$$

where

$$\mu_a = \frac{\delta \mathcal{F}}{\delta n_a} = -\kappa \nabla^2 n_a + \frac{\partial g}{\partial n_a}, \tag{22}$$

is the chemical potential of component a and $M_a = M n_a$ with $M > 0$ specifies the mobility of component a. Our method allows us to explore the dynamics in (21) analytically by observing that the growth of perturbations with wavenumber k around the homogeneous stationary state $n_a^* = \beta/N$ is governed by the Jacobian in equation (6), given by

$$J_{ab}(k) = -J_{ab}^{(2)}k^2 + J_{ab}^{(4)}k^4 = -\frac{\beta}{N}H_{ab}k^2 - \frac{\beta}{N}\kappa\delta_{ab}k^4. \tag{23}$$

Using the same approach as in the proof of Theorem 1, it can be deduced that the real part of the leading eigenvalue $\lambda(k)$ is given by

$$\mathrm{Re}(\lambda(k)) = -k^2\left(\frac{\beta}{N}\kappa k^2 - r_2\right), \tag{24}$$

where r_2 is defined by equation (20) and coincides with the definition in equation (11) (Appendix E). Therefore, in addition to learning that spinodal decomposition occurs when $r_2 > 0$, we also learn that perturbations grow when their wavenumber is in the range of

$$0 < |k| < \sqrt{\frac{Nr_2}{\beta\kappa}}, \tag{25}$$

and the growth is maximal at the wavenumber

$$|k^*| = \sqrt{\frac{Nr_2}{4\beta\kappa}}. \tag{26}$$

Not only does our framework allow for dynamical predictions beyond the standard Landau-Ginzburg theory, but it also provides a simple rule for determining which terms of the free energy functional in equation (16) robustly promote spinodal decomposition. Noticing that the dynamics in equation (21) increases the order of spatial interactions by +2 due to two spatial derivatives, we can classify the spatial interactions straight from the free energy functional in equation (16) as in Fig. 3b. Since the interaction strength of the maximal interaction $r_4 = -\beta\kappa/N$ is negative, Theorem 1 implies that the maximal interaction generated by surface tension cannot in itself generate spinodal decomposition but rather ensures that the spinodal decomposition is regular when generated by other terms (Fig. 3c). Moreover, Theorem 1 also implies that spinodal decomposition occurs when the interaction strength is sufficiently strong ($r_2 \gg 0$, Fig. 3c), which aligns with the more nuanced result in equation (20). Furthermore, if we generalized the surface tension $\kappa > 0$ to a positive definite matrix κ_{ab} via

$$\sum_a \frac{\kappa}{2}(\nabla n_a)^2 \to \sum_{ab}\frac{\kappa_{ab}}{2}\nabla n_a \nabla n_b, \tag{27}$$

then Theorem 1 would imply that the newly introduced maximal cross-interactions of order $p = 4$ with negative strength $r_4 < 0$ would still regularize the spinodal decomposition rather than promote its robustness. Similarly, the addition of symmetric spatial interactions of the form $n_a\nabla n_b$ into the free energy functional in equation (16) would introduce irrelevant interactions of order $p = 3$, meaning that such interactions do not improve the robustness of spinodal decomposition.

On the one hand, Theorem 1 provides a useful guide for constructing models that robustly admit spontaneous pattern formation by identifying appropriate spatial interactions order by order. On the other hand, some spatial interactions inherently carry a multitude of different orders p. Most notably, these interactions include non-local mechanisms, such as cell-cell interactions via pseudopodia in the context of developmental biology [54, 55] or long-range seed dispersal in the context of plant ecology [26, 56]. For example, the models for non-local interactions in [38, 57] have the general form

$$\begin{aligned}\partial_t n_a &= f_a(\mathbf{n}) + d\nabla^2 n_a - \nabla\cdot\boldsymbol{\mathcal{G}}_a[\boldsymbol{n}]\\ \boldsymbol{\mathcal{G}}_a[\boldsymbol{n}] &= G_a(\mathbf{n})\int_{\mathbb{R}^D}\Omega\left(|\boldsymbol{x}|\right)H_a(\mathbf{n})\hat{\mathbf{x}}\mathrm{d}\mathbf{x}^D,\end{aligned} \tag{28}$$

where $d > 0$ is diffusivity, $G_a(\mathbf{n})$ and $H_a(\mathbf{n})$ modify the interaction strength, $\Omega(\boldsymbol{x})$ is the interaction kernel and $\hat{\mathbf{x}}$ is the unit vector of a specified direction in the D-dimensional space $\mathbb{R}^D$. As proved in [38], the Jacobian matrix of equation (6) is given by

$$J_{ab}(k) = J_{ab} - d\delta_{ab}k^2 + \Lambda_{ab}K(k), \tag{29}$$

where $k = |\boldsymbol{k}|$ is the magnitude of the wavenumber vector, the strength of the non-local interactions is captured by the matrix

$$\Lambda_{ab} = \frac{2\pi^{D/2}}{\Gamma\left(\frac{D}{2}\right)}G_a(\mathbf{n}^*)\left.\frac{\partial H_a}{\partial n_b}\right|_{\mathbf{n}^*}, \tag{30}$$

and $K(k)$ is the transformed interaction kernel

$$K(k) = k\int_0^\infty x^{D-1}\Omega(x)j_1^{(D)}(kx)\mathrm{d}x, \tag{31}$$

with $j_1^{(D)}(s)$ being the D-dimensional hyperspherical Bessel function. Since these hyperspherical Bessel functions are odd and analytic, the function $K(k)$ is even and analytic, implying the corresponding term of the Jacobian in equation (29) includes interactions of infinitely many even orders p. For example, if $\Omega(x) = e^{-x}$ and two spatial dimensions are considered ($D = 2$), then the transformed interaction kernel is [38]

$$K(k) = \frac{k^2}{(1+k^2)^{\frac{3}{2}}} = \sum_{p\text{ even}}\binom{-\frac{3}{2}}{\frac{p}{2}}k^{p+2}. \tag{32}$$

If we used Theorem 1 heuristically, this observation would imply that non-local interactions include infinitely many relevant interactions and pattern formation is robust (Fig. 4a). While these interactions are not independent, as assumed in Theorem 1, and are related to the same matrix Λ_{ab}, the steps in the proof of Theorem 1 (Appendix A) can still be used. When the interactions Λ_{ab} are independent and identically distributed with

$$\begin{aligned} a = b: &\quad \mathbb{E}\,\Lambda_{ab} = \mu_s, \quad \mathrm{Var}\,\Lambda_{ab} = \sigma_s^2,\\ a \neq b: &\quad \mathbb{E}\,\Lambda_{ab} = \mu_c, \quad \mathrm{Var}\,\Lambda_{ab} = \sigma_c^2,\\ &\mathrm{Cov}(\Lambda_{ab}, \Lambda_{ba}) = \tau \end{aligned} \tag{33}$$

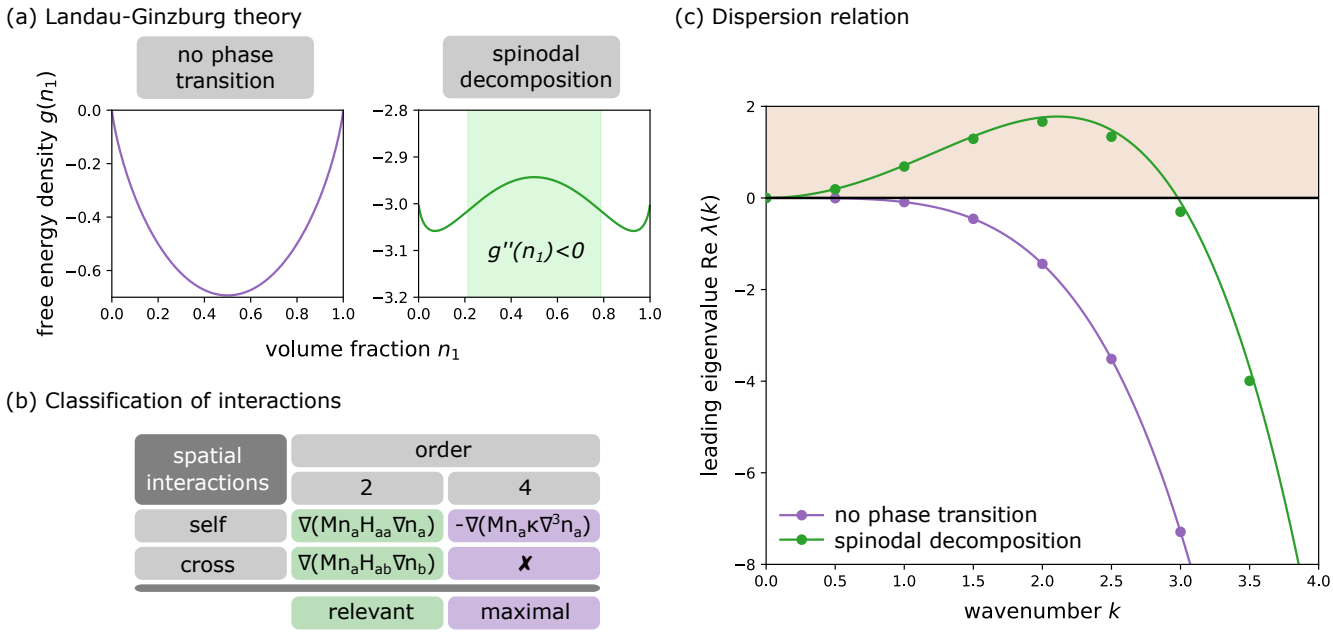

FIG. 3. **Example 2: Spinodal decomposition (a)** Landau-Ginzburg theory predicts whether a well-mixed fluid mixture spontaneously decomposes (spinodal decomposition) based on the free energy density $g(\boldsymbol{n})$ in equation (17), depicted for a binary mixture ($N = 2$) with $n_1 + n_2 = 1$ and interactions $\chi_{ab} = \frac{\nu}{2}(1+\delta_{ab})$ ($\nu = 0$ left, $\nu = 3$ right). Spinodal decomposition is expected to occur if the Hessian matrix has a negative eigenvalue (i.e. $g''(n_1) < 0$, light green region around the maximum of the right panel). **(b)** Interactions in equation (21) are classified as relevant (green; interactions between mixture components) and maximal (purple; surface tension κ). **(c)** Dispersion relations for a multi-component fluid mixture ($N = 1000$) around an equimolar homogeneous stationary state $n_a^* = \beta/N$ with $\beta = 0.9$ in the absence (purple dots and line) and presence (green dots and line) of unstructured symmetric interactions between different components ($\tau_p = 1$). Lines plot the analytics in equation (A7). Symbols represent numerical simulations of the Jacobian matrix in equations (18), (19) and (23), where entries are sampled independently from a Gaussian distribution with a mean $\nu_c = \nu_s = -6$ and a standard deviation $\sigma_s = \sigma_c = \sqrt{N}$, and the surface tension is chosen to be $\kappa = N/10$. The brown region denotes robust pattern formation. See Supplemental Material for the Python code.

and the number of interacting variables N is large, the leading eigenvalue $\lambda(k)$ of the Jacobian matrix in equation (29) is given by

$$\begin{aligned}\mathrm{Re}(\lambda(k)) = \mu_{s0} - \mu_{c0} - dk^2 + (\mu_s - \mu_c)K(k) + \\ + \max\Bigg(N\left[\mu_{c0} + \mu_c K(k)\right], \\ \sqrt{N}\frac{\sigma_{c0}^2(1+\tau_0) + \sigma_c^2 K(k)^2(1+\tau)}{\sqrt{\sigma_{c0}^2 + \sigma_c^2 K(k)^2}}\Bigg),\end{aligned} \tag{34}$$

as proved in Appendix F. Assuming that $K(k) \to 0$ as $k \to \infty$ (which is true for the commonly studied interaction kernels [38]), the value of $\mathrm{Re}(\lambda(k))$ remains bounded from above by 0 as $k \to \infty$ and any spontaneous pattern formation must be regular. Moreover, since there exists a wavenumber k and a sign $s = \pm 1$ such that $sK(k) > 0$, it is always possible to make the strength of non-local interactions

$$r \equiv (\mu_s - \mu_c)s + \max\left(N\mu_c s, \sqrt{N}\sigma_c(1+\tau)\right), \tag{35}$$

sufficiently large so that $\mathrm{Re}(\lambda(k))$ is positive. Put differently, sufficiently strong non-local interactions can always robustly and regularly generate patterns (Fig. 4b), which aligns with our intuition based on the heuristic application of Theorem 1. Further analysis shows that the maximally growing perturbation has a wavenumber that can be approximated by the maximum of the transformed interaction kernel $|K(k)|$ (Appendix F, Fig. 4b), further supporting the intuition that the non-locality of spatial interactions is the key ingredient for robust pattern formation in equation (28). These results generalize previous work that focused on pattern formation with multiplicative noise in the restricted case with $G_a = H_a = n_a$ [57] and provides a key analytical insight into the improved robustness of pattern formation when non-local interactions are compared to reaction-advection-diffusion systems [38].

In this Letter, we have formalized the concept of robust pattern formation (Fig. 1) and illustrated this concept across a variety of models from mathematical biology (Fig. 2, 4) and soft condensed matter physics (Fig. 3). At a conceptual level, our approach shares similarities with the renormalization group in statistical and quantum field theories. While the renormalization group identifies field interactions that are relevant for the physics at

(a) Classification of interactions

spatial interactions	order		
	2	4	p even
self	$(\Lambda_{aa}\text{-}d)k^2$	$-\frac{3}{2}\Lambda_{aa}k^4$	$\binom{-3/2}{p/2}\Lambda_{aa}k^{p+2}$
cross	$\Lambda_{ab}k^2$	$-\frac{3}{2}\Lambda_{ab}k^4$	$\binom{-3/2}{p/2}\Lambda_{ab}k^{p+2}$
	relevant		

(b) Dispersion relation

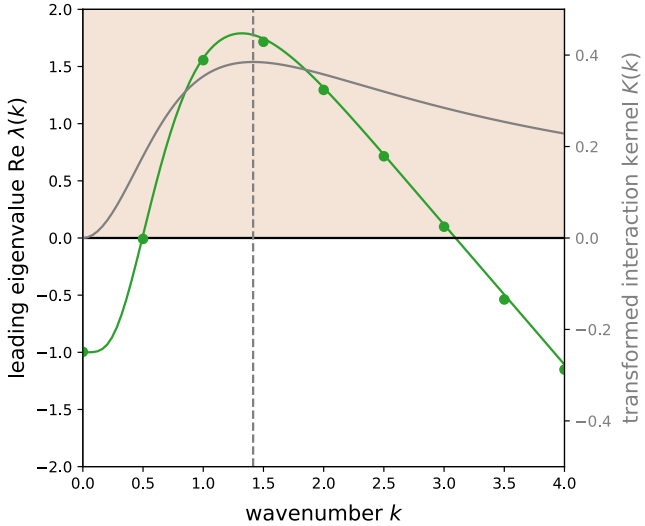

FIG. 4. **Example 3: Nonlocal interactions.** **(a)** Non-local interactions in equation (29) are all relevant when the transformed interaction kernel is expanded in the powers of the wavenumber k. The interaction kernel $K(k)$ in equation (32) is considered for illustration. **(b)** Dispersion relations for non-local interactions in a large system ($N = 1000$) with unstructured interactions ($\tau_p = 0$). The green line corresponds to the analytics in equation (34). The green dots represent numerical simulations of the Jacobian matrix in equation (29) and (33), where entries are sampled independently from Gaussian distributions with means $\mu_{s0} = 2$, $\mu_{c0} = \mu = 0$ and standard deviations $\sigma_{s0} = \sigma_{c0} = 1/\sqrt{N}$, $\sigma = 10/\sqrt{N}$ and the diffusion is chosen to be $d = 0.1$. The brown region denotes robust pattern formation. See Supplemental Material for the Python code. The dispersion relation is overlaid with the transformed interaction kernel $K(k)$ in equation (32) (solid gray line) and its global maximum at $k = \sqrt{2}$ (dashed gray line), which approximately matches the maximum in the dispersion relation.

large length scales, our method (Theorems 1 and 2) identifies interactions that are relevant for robust pattern formation. This approach allows one to formalize the observation that diffusion alone does not generate patterns robustly in large and unstructured systems [23, 31, 33] and that advection [17, 34], chemotaxis [35], cross-diffusion [36] and non-local interactions [37, 38] indeed facilitate pattern formation more robustly than diffusion (Fig. 2, 4). Moreover, our method can be used to explain the robustness of spinodal decomposition in soft condensed matter and analyze its dynamics beyond the regimes predicted from Landau-Ginzburg theory (Fig. 3). Our new tool can also offer a simple guide for creating mathematical models that explain pattern formation in highly complex physical systems [3–6, 21, 22]. Since physical systems can be potentially described by a large number of variables N, the systems that form patterns must either include relevant spatial interactions as outlined in Theorem 1 or have highly correlated and structured interactions. For example, if diffusion is the only mechanism at play, patterns can form in systems with a large number of variables N only if these systems are structured into activator and inhibitor subsystems [29, 58, 59], which might explain the complications with observing Turing patterns in real physical systems [28]. When a complex empirical system forms patterns and there is no apparent interaction structure, Theorem 1 lists spatial interactions that could robustly generate these patterns and can provide a guide for further empirical tests. Altogether, our work defined and examined the robustness of pattern formation in realistically complex systems, providing a map for searching specific mechanisms that generate these spatial patterns.

This work was supported by Oxford Mathematical Institute Scholarship (V.P.). For the purpose of Open Access, the author has applied a CC BY public copyright licence to any Author Accepted Manuscript (AAM) version arising from this submission.

[1] W. P. Wolf, The Ising model and real magnetic materials, Braz. J. Phys. **30**, 794 (2000).
[2] M. Merle, L. Messio, and J. Mozziconacci, Turing-like patterns in an asymmetric dynamic Ising model, Phys Rev E **100**, 042111 (2019).
[3] J. Horváth, I. Szalai, and P. De Kepper, An experimental design method leading to chemical Turing patterns, Science **324**, 772 (2009).
[4] J. B. Xavier, E. Martinez-Garcia, and K. R. Foster, Social evolution of spatial patterns in bacterial biofilms: when conflict drives disorder, Am. Nat. **174**, 1 (2009).
[5] A. Nakamasu, G. Takahashi, A. Kanbe, and S. Kondo, Interactions between zebrafish pigment cells responsible for the generation of Turing patterns, Proc. Natl. Acad. Sci. U. S. A. **106**, 8429 (2009).
[6] M. Rietkerk, S. C. Dekker, P. C. de Ruiter, and J. van de Koppel, Self-organized patchiness and catastrophic shifts in ecosystems, Science **305**, 1926 (2004).
[7] T. Padmanabhan, *Structure Formation in the Universe* (Cambridge University Press, 1993).

[8] J. A. Heras, Can Maxwell's equations be obtained from the continuity equation?, arXiv [physics.class-ph] (2008).

[9] P. Niyogi, *Introduction to Computational Fluid Dynamics* (Pearson Education, Philadelphia, PA, 2006).

[10] G. I. Ogilvie, Astrophysical fluid dynamics, J. Plasma Phys. **82**, 205820301 (2016).

[11] S. M. Allen and J. W. Cahn, A correction to the ground state of FCC binary ordered alloys with first and second neighbor pairwise interactions, Scr. Metall. **7**, 1261 (1973).

[12] M. E. Cates and E. Tjhung, Theories of binary fluid mixtures: from phase-separation kinetics to active emulsions, Journal of Fluid Mechanics **836**, P1 (2018).

[13] A. Schild, Time in quantum mechanics: A fresh look at the continuity equation, arXiv [physics.chem-ph] (2018).

[14] D. V. Widder, *The heat equation*, Pure and Applied Mathematics (Amsterdam) (Academic Press, San Diego, CA, 1976).

[15] I. Lengyel and I. R. Epstein, A chemical approach to designing turing patterns in reaction-diffusion systems, Proc. Natl. Acad. Sci. U. S. A. **89**, 3977 (1992).

[16] J. D. Murray, *Mathematical Biology II* (Springer New York, 2003).

[17] H. Y. Lee and M. Kardar, Macroscopic equations for pattern formation in mixtures of microtubules and molecular motors, Phys. Rev. E Stat. Nonlin. Soft Matter Phys. **64**, 056113 (2001).

[18] J. M. Horowitz and M. Kardar, Bacterial range expansions on a growing front: Roughness, fixation, and directed percolation, Phys. Rev. E. **99**, 042134 (2019).

[19] A. M. Turing, The chemical basis of morphogenesis, Bull. Math. Biol. **52**, 153 (1990).

[20] Editorial, Turing patterns, 70 years later, Nat Comput Sci **2**, 463 (2022).

[21] P. K. Becker and R. J. Field, Stationary concentration patterns in the oregonator model of the Belousov-Zhabotinskii reaction, J. Phys. Chem. **89**, 118 (1985).

[22] A. B. Rovinskii, Turing bifurcation and stationary patterns in the ferroin-catalyzed Belousov-Zhabotinskii reaction, J. Phys. Chem. **91**, 4606 (1987).

[23] P. A. Haas and R. E. Goldstein, Turing's diffusive threshold in random Reaction-Diffusion systems, Phys. Rev. Lett. **126**, 238101 (2021).

[24] L. Hall-Stoodley, J. W. Costerton, and P. Stoodley, Bacterial biofilms: from the natural environment to infectious diseases, Nat. Rev. Microbiol. **2**, 95 (2004).

[25] H. Yamanaka and S. Kondo, In vitro analysis suggests that difference in cell movement during direct interaction can generate various pigment patterns in vivo, Proc. Natl. Acad. Sci. U. S. A. **111**, 1867 (2014).

[26] Y. Pueyo, S. Kefi, C. L. Alados, and M. Rietkerk, Dispersal strategies and spatial organization of vegetation in arid ecosystems, Oikos **117**, 1522 (2008).

[27] M. J. Beck and S. B. Vander Wall, Seed dispersal by scatter-hoarding rodents in arid environments, J. Ecol. **98**, 1300 (2010).

[28] S. T. Vittadello, T. Leyshon, D. Schnoerr, and M. P. H. Stumpf, Turing pattern design principles and their robustness, Philos. Trans. A Math. Phys. Eng. Sci. **379**, 20200272 (2021).

[29] E. Villar-Sepúlveda and A. R. Champneys, General conditions for Turing and wave instabilities in reaction-diffusion systems, J. Math. Biol. **86**, 39 (2023).

[30] N. S. Scholes, D. Schnoerr, M. Isalan, and M. P. H. Stumpf, A comprehensive network atlas reveals that Turing patterns are common but not robust, Cell Syst. **9**, 243 (2019).

[31] H. S. Ahmad Shaberi, A. Kappassov, A. Matas-Gil, and R. G. Endres, Optimal network sizes for most robust Turing patterns, bioRxiv (2024).

[32] R. M. May, Will a large complex system be stable?, Nature **238**, 413 (1972).

[33] R. H. Pazuki and R. G. Endres, Robustness of Turing models and gene regulatory networks with a sweet spot, Phys. Rev. E. **109**, 064305 (2024).

[34] A. B. Rovinsky and M. Menzinger, Chemical instability induced by a differential flow, Phys. Rev. Lett. **69**, 1193 (1992).

[35] E. F. Keller and L. A. Segel, Model for chemotaxis, J. Theor. Biol. **30**, 225 (1971).

[36] V. K. Vanag and I. R. Epstein, Cross-diffusion and pattern formation in reaction–diffusion systems, Phys. Chem. Chem. Phys. **11**, 897 (2009).

[37] K. J. Painter, J. M. Bloomfield, J. A. Sherratt, and A. Gerisch, A nonlocal model for contact attraction and repulsion in heterogeneous cell populations, Bull. Math. Biol. **77**, 1132 (2015).

[38] T. J. Jewell, A. L. Krause, P. K. Maini, and E. A. Gaffney, Patterning of nonlocal transport models in biology: The impact of spatial dimension, Math. Biosci. **366**, 109093 (2023).

[39] Y. Ahmadian, F. Fumarola, and K. D. Miller, Properties of networks with partially structured and partially random connectivity, Phys. Rev. E Stat. Nonlin. Soft Matter Phys. **91**, 012820 (2015).

[40] I. A. Hatton, O. Mazzarisi, A. Altieri, and M. Smerlak, Diversity begets stability: Sublinear growth and competitive coexistence across ecosystems, Science **383**, eadg8488 (2024).

[41] S. Cure and I. Neri, Antagonistic interactions can stabilise fixed points in heterogeneous linear dynamical systems, SciPost Phys. **14** (2023).

[42] K. Z. Coyte, J. Schluter, and K. R. Foster, The ecology of the microbiome: Networks, competition, and stability, Science **350**, 663 (2015).

[43] D. Gravel, F. Massol, and M. A. Leibold, Stability and complexity in model meta-ecosystems, Nat. Commun. **7**, 12457 (2016).

[44] A. Stevens and H. G. Othmer, Aggregation, blowup, and collapse: The ABC's of taxis in reinforced random walks, SIAM J. Appl. Math. **57**, 1044 (1997).

[45] G. Arumugam and J. Tyagi, Keller-segel chemotaxis models: A review, Acta Appl. Math. **171**, 1 (2021).

[46] E. P. Zemskov, K. Kassner, M. A. Tsyganov, and M. J. B. Hauser, Wavy fronts in reaction-diffusion systems with cross advection, Eur. Phys. J. B **72**, 457 (2009).

[47] Y. Maimaiti and W. Yang, Stability and pattern formation in a general class of reaction-diffusion-advection system, Acta Appl. Math. **185**, 1 (2023).

[48] J. Berry, C. P. Brangwynne, and M. Haataja, Physical principles of intracellular organization via active and passive phase transitions, Rep. Prog. Phys. **81**, 046601 (2018).

[49] S. Mao, D. Kuldinow, M. P. Haataja, and A. Košmrlj, Phase behavior and morphology of multicomponent liquid mixtures, Soft Matter **15**, 1297 (2019).

[50] R. P. Sear and J. A. Cuesta, Instabilities in complex mixtures with a large number of components, Phys. Rev.

Lett. **91**, 245701 (2003).

[51] W. M. Jacobs and D. Frenkel, Phase transitions in biological systems with many components, Biophys. J. **112**, 683 (2017).

[52] K. Shrinivas and M. P. Brenner, Phase separation in fluids with many interacting components, Proc. Natl. Acad. Sci. U. S. A. **118**, e2108551118 (2021).

[53] I. R. Graf and B. B. Machta, Thermodynamic stability and critical points in multicomponent mixtures with structured interactions, Phys. Rev. Res. **4**, 033144 (2022).

[54] R. P. Tucker and C. A. Erickson, The control of pigment cell pattern formation in the california newt, taricha torosa, J. Embryol. Exp. Morphol. **97**, 141 (1986).

[55] C. Carmona-Fontaine, H. K. Matthews, S. Kuriyama, M. Moreno, G. A. Dunn, M. Parsons, C. D. Stern, and R. Mayor, Contact inhibition of locomotion in vivo controls neural crest directional migration, Nature **456**, 957 (2008).

[56] J. J. R. Bennett and J. A. Sherratt, Long-distance seed dispersal affects the resilience of banded vegetation patterns in semi-deserts, J. Theor. Biol. **481**, 151 (2019).

[57] F. Olmeda and S. Rulands, Long-range interactions and disorder facilitate pattern formation in spatial complex systems, arXiv [physics.bio-ph] (2023).

[58] R. A. Satnoianu, M. Menzinger, and P. K. Maini, Turing instabilities in general systems, J. Math. Biol. **41**, 493 (2000).

[59] J. W. Baron and T. Galla, Dispersal-induced instability in complex ecosystems, Nat. Commun. **11**, 6032 (2020).

[60] J. W. Baron, T. J. Jewell, C. Ryder, and T. Galla, Eigenvalues of random matrices with generalized correlations: A path integral approach, Phys. Rev. Lett. **128**, 120601 (2022).

[61] H. Nguyen and S. O'Rourke, The elliptic law, arXiv [math.PR] (2012).

Appendix A: Proof of Theorem 1

Equations (6) and (9) imply that the on-diagonal and off-diagonal entries of the matrix $J_{ab}(k)$ are independent and identically distributed with

$$\begin{aligned} \mathbb{E}\, J_{ab}(k) &= \sum_{p=0}^{\infty}[\mu_{sp}\delta_{ab} + \mu_{cp}(1-\delta_{ab})](ik)^p, \\ \operatorname{Var} J_{ab} &= \sum_{p=0}^{\infty}[\sigma_{sp}^2\delta_{ab} + \sigma_{cp}^2(1-\delta_{ab})]k^{2p}, \end{aligned} \tag{A1}$$

where the entries are independent up to a correlation between opposite entries across the diagonal, described by the pseudo-covariance

$$\operatorname{Cov}\left(J_{ab}(k), \overline{J_{ba}(k)}\right) = \sum_{p=0}^{\infty}(-1)^p\tau_p\sigma_{cp}^2k^{2p}. \tag{A2}$$

Since the off-diagonal entries generally have non-zero means, $J_{ab}(k)$ has a single outlier eigenvalue [60], given by

$$\lambda_o(k) = \sum_{p=0}^{\infty}\mu_{sp}(ik)^p + (N-1)\sum_{p=0}^{\infty}\mu_{cp}(ik)^p. \tag{A3}$$

The distribution of the remaining eigenvalues can be determined by a rank-one perturbation approach, as in [40]. Specifically, the eigenvalues of the matrix $J_{ab}(k)$ have the same distribution as the eigenvalues of the matrix $J_{ab}(k) - \mathbb{E}\, J_{ab}(k)$, up to a shift by

$$c(k) = \sum_{p=0}^{\infty}[\mu_{sp} - \mu_{cp}](ik)^p, \tag{A4}$$

and the eigenvalues of the matrix $J_{ab}(k) - \mathbb{E}\, J_{ab}(k)$ are distributed uniformly in an ellipse [61] with a half-width $a_+(k)$ (resp. half-height $a_-(k)$) given by

$$a_\pm(k) = \frac{N\sum_{p=0}^{\infty}\sigma_{cp}^2(1\pm(-1)^p\tau_p)k^{2p}}{\sqrt{N\sum_{p=0}^{\infty}\sigma_{cp}^2k^{2p}}}. \tag{A5}$$

Therefore, the bulk of the eigenvalues of $J_{ab}(k)$ are distributed in an ellipse with center $c(k)$, half-width $a_+(k)$ and half-height $a_-(k)$, implying that the eigenvalue in the bulk spectrum with the maximal real part is given by

$$\lambda_b(k) = c(k) + a_+(k). \tag{A6}$$

Thus, the eigenvalue with the maximal real part $\lambda(k)$ is given by $\lambda_o(k)$ (resp. $\lambda_b(k)$) if $\mathrm{Re}\lambda_o(k) > \mathrm{Re}\lambda_b(k)$ (resp. $\mathrm{Re}\lambda_o(k) < \mathrm{Re}\lambda_b(k)$) and the corresponding maximal real part is

$$\mathrm{Re}\lambda(k) = \sum_{p\text{ even}}(\mu_{sp} - \mu_{cp})(-1)^{\frac{p}{2}}k^p + \max\left(N\sum_{p\text{ even}}\mu_{cp}(-1)^{\frac{p}{2}}k^p, a_+(k)\right). \tag{A7}$$

If the only interactions present had order p, then equation (A7) would imply that

$$\mathrm{Re}\lambda(1) = r_p, \tag{A8}$$

where r_p is the interaction strength of order p in equations (11) and (12) of Definition 1. Therefore, the sign of the interaction strength r_p in Definition 1 determines whether all eigenvalues of the matrix $i^pJ_{ab}^{(p)}$ have negative real parts ($r_p < 0$) or not ($r_p > 0$). In particular, since we assume that the homogeneous stationary state is stable, it must be true that all eigenvalues of $J_{ab}^{(0)}$ have negative real parts and $r_0 < 0$. With these relationships, we can prove the respective statements in Theorem 1:

1. We can notice that the equation (A7) does not include μ_{sp}, μ_{cp} and σ_{sp}^2 for any self-interaction of any odd order p. Moreover, for any odd order p with $\tau_p = 1$, $\mathrm{Re}\lambda(k)$ decreases with increasing σ_{cp}^2, as can be deduced from equation (A5). Therefore, pattern formation is not robust when irrelevant interactions are the only interactions present since

$$\mathrm{Re}\lambda(k) \leq \mathrm{Re}\lambda(0) = r_0 < 0 \tag{A9}$$

for any wavenumber k.

2. When there is at least one significant interaction of order $p > P$ with non-vanishing strength $r_p \neq 0$, equations (A7) and (A5) imply that

$$\mathrm{Re}\lambda(k) \sim r_p |k|^p \tag{A10}$$

as $|k| \to \infty$, where p corresponds to the maximal order among all such significant interactions. Since $r_p \geq 0$ by equation (12), the presence of significant interactions makes pattern formation robust and irregular.

3. When all significant interactions have vanishing strength and the relevant interactions are absent, there are two cases that depend on the strength of the maximal interaction r_P, given by equation (11).

   (a) When $r_P > 0$, the substitution of equations (11) and (A5) into (A7) imply that

$$\mathrm{Re}\lambda(k) \sim r_P |k|^P \tag{A11}$$

   as $|k| \to \infty$ and pattern formation is robust and irregular.

   (b) When $r_P \leq 0$, equation (11) implies that

$$\begin{aligned} 0 &\geq [\mu_{sp} + (N-1)\mu_{cp}](-1)^{\frac{p}{2}}, \\ 0 &\geq (\mu_{sp} - \mu_{cp})(-1)^{\frac{p}{2}} + \sqrt{N}\sigma_{cp}\,[1+\tau_p] \end{aligned} \tag{A12}$$

   for $p = P$. Equation (A12) is also true for $p = 0$ (with strict inequalities) due to the stability of the homogeneous stationary state ($r_0 < 0$). Therefore, using equation (A12) for $p = 0, P$, we find that equation (A3) for the outlier eigenvalue satisfies

$$\mathrm{Re}\,\lambda_o(k) = \sum_{p=0,P} [\mu_{sp} + (N-1)\mu_{cp}](-1)^{\frac{p}{2}} k^p < 0, \tag{A13}$$

   and equation (A6) for the eigenvalues in the bulk spectrum satisfies

$$\begin{aligned} \mathrm{Re}\,\lambda_b(k) = \mathrm{Re}(c(k) + a_+(k)) &= \sum_{p=0,P} (\mu_{sp} - \mu_{cp})(-1)^{\frac{p}{2}} k^p + \frac{\sqrt{N}\sum_{p=0,P}\sigma_{cp}^2(1+\tau_p)k^{2p}}{\sqrt{\sum_{p=0,P}\sigma_{cp}^2 k^{2p}}} \\ &< \sqrt{N}\frac{\sum_{p=0,P}\sigma_{cp}(1+\tau_p)k^p[\sigma_{cp}^2 k^p - \sqrt{\sigma_{c0}^2 + \sigma_{cP}^2 k^{2P}}]}{\sqrt{\sigma_{c0}^2 + \sigma_{cP}^2 k^{2P}}} \leq 0. \end{aligned} \tag{A14}$$

   for any wavenumber k. Therefore, equations (A13) and (A14) imply that the maximal real part of any eigenvalue satisfies

$$\mathrm{Re}\,\lambda(k) = \max\left[\mathrm{Re}\,\lambda_o(k), \mathrm{Re}\,\lambda_b(k)\right] < 0. \tag{A15}$$

   for any wavenumber k, meaning that pattern formation is not robust according to Definition 2.

4. If we fix some wavenumber k^* and some relevant interaction of order p, we can make the interaction strength sufficiently strong ($r_p \gg 0$) so that

$$\mathrm{Re}\lambda(k^*) \approx r_p |k^*|^p > 0, \tag{A16}$$

implying that pattern formation is robust for sufficiently strong relevant interactions. Moreover, when all significant interactions have vanishing strength and the maximal interaction has negative strength, equation (A11) is valid asymptotically at large k and pattern formation is regular.

Appendix B: Proof of Theorem 2

To prove Theorem 2, we treat particular realizations $J_{ab}^{(p)}$ of the spatial interactions $p \geq 1$ as deterministic matrices and the matrix of temporal interactions $J_{ab}^{(0)}$ as a sum of a diagonal deterministic matrix and a non-diagonal random matrix, as in equation (9) with $\tau_0 = \mu_{c0} = 0$. Assuming that the only spatial interactions are self-interactions (i.e., $J_{ab}^{(p)}$ are diagonal matrices), the Jacobian matrix in equation (6) can be written as

$$J_{ab}(k) = \delta_{ab} \sum_{p=0}^{\infty} J_{aa}^{(p)} (ik)^p + (1 - \delta_{ab}) J_{ab}^{(0)}, \tag{B1}$$

where the first term corresponds to a deterministic diagonal matrix and the second term corresponds to an off-diagonal stochastic matrix. Using the result in [39], the eigenvalues of the Jacobian matrix $J_{ab}(k)$ are distributed within a region of the complex plane $z \in \mathbb{C}$, given by

$$f(z,k) \equiv \sum_{a=1}^{N} \frac{1}{\left| z - \sum_{p=0}^{\infty} J_{aa}^{(p)} (ik)^p \right|^2} \geq \frac{1}{\sigma_{c0}^2}. \tag{B2}$$

Since the temporal dynamics is assumed to be stable in the absence of spatial interactions, the region given by equation (B2) lies in the real negative half-plane $\{\mathrm{Re}(z) < 0\}$ when $k = 0$. Specifically, this implies that $J_{aa}^{(0)} < 0$ for all a.

With these relationships, we can prove the respective statements in Theorem 2:

1. When the irrelevant interactions are the only interactions present, we can use the inequality $|z| \geq |\mathrm{Re}(z)|$ to note that

$$\left| z - \sum_{p=0}^{\infty} J_{aa}^{(p)} (ik)^p \right| = \left| z - J_{aa}^{(0)} - \sum_{p \text{ odd}} J_{aa}^{(p)} (ik)^p \right| \geq \left| \mathrm{Re}(z) - J_{aa}^{(0)} \right| \tag{B3}$$

   for every field variable with index a. Therefore,

$$f(\mathrm{Re}(z), 0) \geq f(z,k) \geq \frac{1}{\sigma_{c0}^2}, \tag{B4}$$

   meaning that, if z lies in the eigenvalue region given by equation (B2) for some $k \neq 0$, then $\mathrm{Re}(z)$ lies in this eigenvalue region for $k = 0$. Since all eigenvalues have negative real parts at $k = 0$, this observation implies that all eigenvalues have negative real parts at all wavenumbers k. Put differently, pattern formation is not robust.

2. When all relevant interactions are absent, there are two cases depending on the signs of the maximal interactions $J_{aa}^{(P)}$, where we recall that P is even by Definition 1.

   (a) If $J_{aa}^{(P)} (-1)^{\frac{P}{2}} \leq 0$ for all a, we start by considering a case where all irrelevant interactions are absent. In this case, the function $f(z, k^2)$ in equation (B2) only includes the power k^P and

$$\frac{\partial f}{\partial k^P} = 2 \sum_{a=1}^{N} \frac{(-1)^{\frac{P}{2}} J_{aa}^{(P)} \left[\mathrm{Re}(z) - J_{aa}^{(0)} - (-1)^{\frac{P}{2}} J_{aa}^{(P)} k^P \right]}{\left| z - J_{aa}^{(0)} - (-1)^{\frac{P}{2}} J_{aa}^{(P)} k^P \right|^4} \leq 0 \tag{B5}$$

   for any z with a positive real part, since $J_{aa}^{(P)} (-1)^{\frac{P}{2}} \leq 0$ and $J_{aa}^{(0)} < 0$ by assumption. This observation implies that, for any wavenumber k,

$$f(z,k) \leq f(z,0) \leq \frac{1}{\sigma^2}, \tag{B6}$$

   where the second inequality follows from the fact that the eigenvalues have negative real parts at $k = 0$. Therefore, the eigenvalue region in equation (B2) lies in the negative real half plane for any wavenumber k and pattern formation is not robust. To extend this result to cases where irrelevant interactions are present, we can prove that a system with irrelevant interactions has at least one eigenvalue with a positive real part only if there is an eigenvalue with a positive real part in the system that has the irrelevant interactions

removed. To prove this statement, we can use the inequality $|z| \geq |\operatorname{Re}(z)|$ so that

$$\left| z - \sum_{p=0}^{\infty} J_{aa}^{(p)} (ik)^p \right| \geq \left| \operatorname{Re}(z) - \sum_{p \text{ even}} J_{aa}^{(p)} (ik)^p \right|. \tag{B7}$$

Defining

$$g(z,k) \equiv \sum_{a=1}^{N} \frac{1}{\left| z - \sum_{p \text{ even}} J_{aa}^{(p)} (ik)^p \right|^2}. \tag{B8}$$

to be the function as in equation (B2)but for a system where the irrelevant interactions are removed, equation (B7) implies that

$$g\left(\operatorname{Re}(z), k\right) \geq f(z,k) \geq \frac{1}{\sigma_{c0}^2}, \tag{B9}$$

where $f(z,k)$ is still given by equation (B2) and describes the system where irrelevant interactions are present. Therefore, if the eigenvalue region in equation (B2) for the system with irrelevant interactions (described by function f) contains a number z with a positive real part, then the positive number $\operatorname{Re}(z)$ is included in the eigenvalue region of the system that has the irrelevant interactions removed (described by function g). But, as we have just shown, such a system only has eigenvalues with negative real parts. Therefore the statement (a) of Theorem 2 applies even if irrelevant interactions are present.

(b) When $J_{aa}^{(P)} (-1)^{\frac{P}{2}} > 0$ for some a, then the region given by equation (B2) includes the circle

$$\left| z - J_{aa}^{(0)} - (-1)^{\frac{P}{2}} J_{aa}^{(P)} k^P \right|^2 \leq \sigma_{c0}^2 \tag{B10}$$

centred at

$$J_{aa}^{(0)} + (-1)^{\frac{P}{2}} J_{aa}^{(P)} k^P, \tag{B11}$$

which is positive for any sufficiently large $|k|$ because $(-1)^{\frac{P}{2}} J_{aa}^{(P)} > 0$ by assumption and P is an even power. Therefore, in this case, pattern formation is robust and irregular.

3. Since the eigenvalue region in equation (B2) includes the circles for each field variable of index a

$$\left| z - \sum_{p=0}^{\infty} J_{aa}^{(p)} (ik)^p \right|^2 \leq \sigma_{c0}^2, \tag{B12}$$

with the real part of the centre located at

$$\sum_{p \text{ even}} (-1)^{\frac{p}{2}} J_{aa}^{(p)} k^p, \tag{B13}$$

sufficiently strong relevant interactions ($J_{aa}^{(p)} (-1)^{\frac{p}{2}} \gg 0$ for some a) can always move this centre to the positive real half plane at any fixed wavenumber k. Therefore, sufficiently strong relevant interactions can always make pattern formation robust as in Definition 2. Moreover, for sufficiently large k,

$$\sum_{p=0}^{\infty} J_{aa}^{(p)} (ik)^p \approx \sum_{p=P}^{\infty} J_{aa}^{(p)} (ik)^p, \tag{B14}$$

and the eigenvalue region in equation (B2) can be approximated by the corresponding eigenvalue region with interactions of order $p < P$ removed, which includes all relevant interactions. When $J_{aa}^{(P)} (-1)^{\frac{P}{2}} < 0$ for all a, the second point of Theorem 2 implies that such a reduced system has only eigenvalues with negative real parts, meaning that all eigenvalues of the full system must have negative real parts at sufficiently large wavenumbers k. Therefore, the resulting pattern formation is robust when $J_{aa}^{(P)} (-1)^{\frac{P}{2}} < 0$ for all a.

Appendix C: Extension to Multiple Spatial Dimensions

In the case of multiple spatial dimensions, the situation is complicated by the fact that the interactions $J_{ab}^{(p),\alpha_1\ldots\alpha_p}$ in equation (6) now have multiple upper spatial indices. Writing $\boldsymbol{\alpha} = (\alpha_1, \ldots, \alpha_p)$, the independent and identical distribution of interactions in equation (9) can be generalized to

$$\begin{aligned} a = b: \ \mathbb{E}\, J_{ab}^{(p),\boldsymbol{\alpha}} &= \mu_{sp\boldsymbol{\alpha}}, \ \ \mathrm{Var}\, J_{ab}^{(p),\boldsymbol{\alpha}} = \sigma_{sp\boldsymbol{\alpha}}^2, \\ a \neq b: \ \mathbb{E}\, J_{ab}^{(p),\boldsymbol{\alpha}} &= \mu_{cp\boldsymbol{\alpha}}, \ \ \mathrm{Var}\, J_{ab}^{(p),\boldsymbol{\alpha}} = \sigma_{cp\boldsymbol{\alpha}}^2, \end{aligned} \tag{C1}$$

and equation (10) to

$$\mathrm{Cov}\left(J_{ab}^{(p),\boldsymbol{\alpha}}, J_{ba}^{(p),\boldsymbol{\alpha}}\right) = \tau_{p\boldsymbol{\alpha}}\sigma_{cp\boldsymbol{\alpha}}^2. \tag{C2}$$

Correspondingly, equations (A1) and (A2) are generalized to

$$\begin{aligned} \mathbb{E}\, J_{ab}(k) &= \sum_{p=0}^{\infty}\sum_{\boldsymbol{\alpha}}[\mu_{sp\boldsymbol{\alpha}}\delta_{ab} + \mu_{cp\boldsymbol{\alpha}}(1-\delta_{ab})]\prod_{q=1}^{p}(ik_{\alpha_q}), \\ \mathrm{Var}\, J_{ab} &= \sum_{p=0}^{\infty}\sum_{\boldsymbol{\alpha}}[\sigma_{sp\boldsymbol{\alpha}}^2\delta_{ab} + \sigma_{cp\boldsymbol{\alpha}}^2(1-\delta_{ab})]\prod_{q=1}^{p}k_{\alpha_q}^2, \end{aligned} \tag{C3}$$

and

$$\mathrm{Cov}\left(J_{ab}(k), \overline{J_{ab}(k)}\right) = \sum_{p=0}^{\infty}\sum_{\boldsymbol{\alpha}}(-1)^p\tau_{p\boldsymbol{\alpha}}\sigma_{cp\boldsymbol{\alpha}}^2\prod_{q=1}^{p}k_{\alpha_q}^2. \tag{C4}$$

With these modifications, one could appropriately modify the subsequent steps in the proof of Theorem 1 (Appendix A) and Theorem 2 (Appendix B) to generalize these results to multiple spatial dimensions.

For illustration, we can notice that Theorem 1 generalizes to an arbitrary number of spatial dimensions D when the interactions are minimally anisotropic, that is, when

$$\begin{aligned} \mu_{sp\boldsymbol{\alpha}} &= \mu_{sp}\frac{2^{\frac{p}{2}}\left(\frac{p}{2}\right)!}{p!}\sum_{\text{pairings } \pi}\prod_{(q_1,q_2)\in\pi}\delta_{\alpha_{q_1}\alpha_{q_2}}, \\ \mu_{cp\boldsymbol{\alpha}} &= \mu_{cp}\frac{2^{\frac{p}{2}}\left(\frac{p}{2}\right)!}{p!}\sum_{\text{pairings } \pi}\prod_{(q_1,q_2)\in\pi}\delta_{\alpha_{q_1}\alpha_{q_2}}, \end{aligned} \tag{C5}$$

for interactions of even order p and

$$\sigma_{sp\boldsymbol{\alpha}}^2 = \sigma_{sp}^2, \ \ \sigma_{cp\boldsymbol{\alpha}}^2 = \sigma_{cp}^2, \ \ \tau_{p\boldsymbol{\alpha}} = \tau_p^2, \tag{C6}$$

for interactions of all orders p. In this case, the key equation (A7) in the proof of Theorem 1 remains valid if we interpret $k = |\boldsymbol{k}|$ as the magnitude of the wavenumber vector $\boldsymbol{k}$. Therefore, Theorem 1 remains valid in arbitrary spatial dimension D under these conditions.

Appendix D: Reaction-Advection-Diffusion Systems

In this section, we analyze the reaction-advection-diffusion system in equations (13), (14) and (15), with the additional assumption that cross-interactions are not constrained by any symmetries, that is $\tau_p = 0$. Under this assumption, the eigenvalue with the maximal real part in equation (A7) becomes

$$\mathrm{Re}\lambda(k) = (\mu_{s0} - \mu_{c0}) - (\mu_{s0} - \mu_{c0})k^2 + \max\left(N[\mu_{c0} - \mu_{c2}k^2], \sqrt{N}\sqrt{\sigma_{c0}^2 + \sigma_{c1}^2k^2 + \sigma_{c2}^2k^4}\right). \tag{D1}$$

When k is large, equation (11) implies that

$$\mathrm{Re}\lambda(k) \approx r_2k^2, \tag{D2}$$

which means that pattern formation is robust and irregular when

$$0 < r_2 \equiv \mathbb{E}\, d_{ab} - n^* \,\mathbb{E}\, c_{ab} - \mathbb{E}\, d_a + \max\left(N[n^* \,\mathbb{E}\, c_{ab} - \mathbb{E}\, d_{ab}], \sqrt{N[\mathrm{Var}\, d_{ab} + (n^*)^2 \,\mathrm{Var}\, c_{ab}]}\right), \tag{D3}$$

that is, when chemotaxis is sufficiently positive ($\mathbb{E}\, c_{ab} \gg 0$), or cross-diffusion sufficiently negative ($\mathbb{E}\, d_{ab} \ll 0$) or either of these is sufficiently heterogeneous ($\mathrm{Var}\, d_{ab}, \mathrm{Var}\, c_{ab} \gg 0$). When $r_2 < 0$, the stability of the homogeneous stationary state implies $r_0 < 0$ (as shown in Appendix A) and we obtain

$$\mu_{s0} - \mu_{s2}k^2 + (N-1)(\mu_{c0} - \mu_{c2}k^2) \leq r_0 + r_2 < 0. \tag{D4}$$

Therefore, pattern formation is robust precisely when

$$f(k^2) = (\mu_{s0} - \mu_{c0}) - (\mu_{s2} - \mu_{c2})k^2 + \sqrt{N}\sqrt{\sigma_{c0}^2 + \sigma_{c1}^2 k^2 + \sigma_{c2}^2 k^4} > 0 \tag{D5}$$

for some wavenumber k, which can be rewritten as

$$\sqrt{N}\sqrt{\sigma_{c0}^2 + \sigma_{c1}^2 k^2 + \sigma_{c2}^2 k^4} > (\mu_{s2} - \mu_{c2})k^2 - (\mu_{s0} - \mu_{c0}) \tag{D6}$$

Since the interaction strengths r_0 and r_2 in equation (11) are assumed to be negative, it is true that

$$(\mu_{s2} - \mu_{c2})k^2 - (\mu_{s0} - \mu_{c0}) > \sqrt{N\sigma_{c2}^2}k^2 + \sqrt{N\sigma_{c0}^2} > 0. \tag{D7}$$

Upon squaring and rearranging the equation (D6), we learn that pattern formation is robust precisely if

$$g(k^2) = \left[N\sigma_{c2}^2 - (\mu_{s2} - \mu_{c2})^2\right] k^4 + \left[N\sigma_{c1}^2 + 2(\mu_{s0} - \mu_{c0})(\mu_{s2} - \mu_{c2})\right] k^2 + N\sigma_{c0}^2 - (\mu_{s0} - \mu_{c0})^2 > 0 \tag{D8}$$

for some wavenumber k. Since the interaction strengths r_0 and r_2 in equation (11) are assumed to be negative, the coefficients at k^4 and k^0 are negative, meaning that the resulting pattern formation is necessarily regular. To determine when this robust and regular pattern formation occurs, we can notice that the function $g(k^2)$ has a maximum at

$$k^2 = \frac{N\sigma_{c1}^2 + 2(\mu_{s0} - \mu_{c0})(\mu_{s2} - \mu_{c2})}{2[(\mu_{s2} - \mu_{c2})^2 - N\sigma_{c2}^2]}, \tag{D9}$$

provided $N\sigma_{c1}^2 > -2(\mu_{s0} - \mu_{c0})(\mu_{s2} - \mu_{c2})$, and $f(k^2)$ is positive at this maximum, provided

$$|N\sigma_{c1}^2 + 2(\mu_{s0} - \mu_{c0})(\mu_{s2} - \mu_{c2})| > 2\sqrt{[(\mu_{s0} - \mu_{c0})^2 - N\sigma_{c0}^2][(\mu_{s2} - \mu_{c2})^2 - N\sigma_{c2}^2]}. \tag{D10}$$

Therefore, there is an intermediate range of wavenumbers k corresponding to growing perturbation modes precisely if

$$N\sigma_{c1}^2 > 2\left(-(\mu_{s0} - \mu_{c0})(\mu_{s2} - \mu_{c2}) + \sqrt{[(\mu_{s0} - \mu_{c0})^2 - N\sigma_{c0}^2][(\mu_{s2} - \mu_{c2})^2 - N\sigma_{c2}^2]}\right), \tag{D11}$$

that is, precisely when the cross-advection is sufficiently heterogeneous (i.e., $\sigma_{c1}^2 \gg 0$). When this condition is satisfied, pattern formation is robust, regular and the maximally growing perturbations have wavenumbers given by equation (D9). In particular, we reproduce the results of Theorem 1 by showing that patterns can be generated robustly by sufficiently strong cross-diffusion, chemotaxis and cross-advection, out of which only cross-advection generates patterns regularly. By performing this more detailed calculation, we additionally obtain the exact conditions for robust pattern formation that is irregular (equation (D3)), and regular (equation (D11)), as well as the critical wavenumber of the fastest growing perturbation for the latter case (equation (D9)).

Appendix E: Spinodal Decomposition of Soft Condensed Matter

In this section, we analyze the spinodal decomposition as described by equations (18), (19) and (23). Upon substituting equation (18) into equation (23) and applying equation (19), we can see that

$$\begin{aligned}
\mathbb{E}\, J_{ab}^{(2)} &= \frac{\beta}{N}\,\mathbb{E}\, H_{ab} = \left(\frac{\beta}{N}\nu_s + 1 + \frac{\beta}{N(1-\beta)}\right)\delta_{ab} + \left(\frac{\beta}{N}\nu_c + \frac{\beta}{N(1-\beta)}\right)(1-\delta_{ab}) \\
\mathrm{Var}\, J_{ab}^{(2)} &= \frac{\beta^2}{N^2}\,\mathrm{Var}\, H_{ab} = \left(\frac{\beta}{N}\sigma_s\right)^2 \delta_{ab} + \left(\frac{\beta}{N}\sigma_c\right)^2 (1-\delta_{ab}) \\
\mathbb{E}\, J_{ab}^{(4)} &= -\frac{\beta}{N}\kappa\delta_{ab} \\
\mathrm{Var}\, J_{ab}^{(4)} &= 0.
\end{aligned} \tag{E1}$$

Substitution of these relationships into equation (A7) reveals that the eigenvalue with the maximal real part $\lambda(k)$ must satisfy

$$\mathrm{Re}\lambda(k) = -k^2\left(\frac{\beta}{N}\kappa k^2 - r_2\right), \tag{E2}$$

where r_2 is given by equation (20). Substitution of these relationships into equation (11) also reveals that r_2 in equation (20) coincides with the interaction strength in Definition 1. Since $\mathrm{Re}\lambda(k)$ is a quadratic function, it is straightforward to deduce that patterns form robustly precisely when $r_2 > 0$. Moreover, such pattern formation is always regular and restricted to wavenumbers in the range of equation (25), with the fastest growing perturbation having a critical wavenumber given by equation (26). Finally, to relate our dynamical approach with the approach of Landau-Ginzburg theory, we note that $r_2 > 0$ precisely when the matrix $-J^{(2)}_{ab}$ has at least one positive eigenvalue (see Appendix A) which, by equation (23), happens precisely when the matrix H_{ab} has at least one negative eigenvalue.

Appendix F: Nonlocal Interactions

In this section, we analyze the model with non-local interactions, as described in equations (29) and (33). Using these equations, we can deduce that

$$\begin{aligned}
\mathbb{E}\, J_{ab}(k) &= \left(\mu_{s0} - dk^2 + \mu_s K(k)\right)\delta_{ab} + \left(\mu_{c0} + \mu_c K(k)\right)(1-\delta_{ab}) \\
\mathrm{Var}\, J_{ab}(k) &= \left(\sigma_{s0}^2 + \sigma_s^2 K(k)^2\right)\delta_{ab} + \left(\sigma_{c0}^2 + \sigma_c^2 K(k)^2\right)(1-\delta_{ab}) \\
\mathrm{Cov}(J_{ab}(k), \overline{J_{ba}(k)}) &= \tau_0\sigma_{c0}^2 + \tau\sigma_c^2 K(k)^2.
\end{aligned} \tag{F1}$$

Assuming that the variance of the diagonal elements is bounded by the variance of the off-diagonal elements as in Theorem 1, we can use the same arguments from random matrix theory as in Appendix A [40, 60, 61] to deduce that the Jacobian matrix $J_{ab}(k)$ has a single outlier eigenvalue

$$\lambda_o(k) = \mu_{s0} - dk^2 + \mu_s K(k) + (N-1)\left(\mu_{c0} + \mu_c K(k)\right) \tag{F2}$$

and a bulk spectrum of eigenvalues, with a point of maximal positive real part that is given by

$$\lambda_b(k) = \mu_{s0} - \mu_{c0} - dk^2 + (\mu_s - \mu_c)\,K(k) + \sqrt{N}\frac{\sigma_{c0}^2(1+\tau_0) + \sigma_c^2 K(k)^2(1+\tau)}{\sqrt{\sigma_{c0}^2 + \sigma_c^2 K(k)^2}}, \tag{F3}$$

for a fixed wavenumber k. Noticing that these eigenvalues are real, we can deduce that the eigenvalue with the maximal real part is given by

$$\lambda(k) = \max(\lambda_o(k), \lambda_b(k)), \tag{F4}$$

which, upon substitution of equations (F2) and (F3), proves equation (34) from the main text. Defining

$$\begin{aligned}
r_0^{(o)} &= \mu_{s0} + (N-1)\mu_{c0} \\
r^{(o)} &= [\mu_s + (N-1)\mu_c]\mathrm{sign}(K(k)) \\
r_0^{(b)} &= \mu_{s0} - \mu_{c0} + \sqrt{N}\sigma_{c0}(1+\tau_0) \\
r^{(b)} &= [\mu_s - \mu_c]\mathrm{sign}(K(k)) + \sqrt{N}\sigma_c(1+\tau),
\end{aligned} \tag{F5}$$

we deduce that the interaction strengths in equations (11) and (20) are given by

$$\begin{aligned}
r_0 &= \max(r_0^{(o)}, r_0^{(b)}) \\
r &= \max(r^{(o)}, r^{(b)})
\end{aligned} \tag{F6}$$

and the eigenvalues in equations (F2) and (F3) are given by

$$\begin{aligned}
\lambda_o(k) &= r_0^{(o)} - dk^2 + r^{(o)}|K(k)| \\
\lambda_b(k) &= r_0^{(b)} - dk^2 + r^{(b)}|K(k)| \\
&\quad - \sqrt{N}\frac{\sigma_{c0}(1+\tau_0)[\sqrt{\sigma_{c0}^2 + \sigma_c^2 K(k)^2} - \sigma_{c0}] + \sigma_c|K(k)|(1+\tau)[\sqrt{\sigma_{c0}^2 + \sigma_c^2 K(k)^2} - \sigma_c|K(k)|]}{\sqrt{\sigma_{c0}^2 + \sigma_c^2 K(k)^2}}.
\end{aligned} \tag{F7}$$

Since the homogeneous stationary state is stable by assumption, we know that $r_0 < 0$, meaning that $r_0^{(o)}, r_0^{(b)} < 0$. Therefore, the leading eigenvalue $\lambda(k)$ is positive precisely when either of $\lambda_o(k)$ and $\lambda_b(k)$ is positive, which happens when $r^{(o)}$ (resp. $r^{(b)}$) is sufficiently large. This argument implies that sufficiently strong non-local interactions with $r \gg 0$ can robustly generate patterns, as presented in the main text. Moreover, when the strength of the non-local interaction $r^{(i)} \gg 0$ is sufficiently strong for $i = o$ (resp. $i = b$), the corresponding eigenvalue in equation (F7) can be approximated by

$$\lambda_i(k) \approx r^{(i)} |K(k)|. \tag{F8}$$

This observation implies that, when patterns form due to the bulk $i = b$ (resp. outlier $i = o$) eigenvalue being positive (i.e., when $r^{(i)} \gg 0$), the critical wavenumber k that maximizes $\lambda_i(k)$ is given by the maximum of $|K(k)|$. Therefore, when patterns form, the critical wavenumber k that maximizes the leading eigenvalue $\lambda(k)$ can be approximated by the maximum of $|K(k)|$, as stated in the main text.